SEDIMENTS, SEC 3 • HILLSLOPE AND RIVER BASIN SEDIMENT DYNAMICS • RESEARCH ARTICLE

The use of visible and near-infrared reflectance measurements for identifying the source of suspended sediment in rivers and comparison with chemical fingerprinting

Dries Verheyen • Jan Diels • Endalkachew Kissi • Jean Poesen

D. Verheyen (✉) • J. Diels • J. Poesen
Department of Earth and Environmental Sciences, KU Leuven, Celestijnenlaan 200 E, 3001 Leuven, Belgium
e-mail: dries.verheyen@ees.kuleuven.be

E. Kissi
Department of Natural Resource Management, School of Agriculture, Jimma University, POB 378, Jimma, Ethiopia

(✉) **Corresponding author:**
Dries Verheyen
Tel.: +3216329754
Fax: +3216329760
e-mail: dries.verheyen@ees.kuleuven.be

Abstract

Purpose - Visible and near-infrared (Vis-NIR) reflectance measurements may be an alternative technique to identify suspended sediment sources in streams of headwater catchments. In this study, we examined if Vis-NIR reflectance measurements are capable of estimating sediment source contribution to sediment yield and compared this technique with the chemical technique.

Materials and methods - Two headwater catchments in Ethiopia, Unta (2052 ha) and Desera (1657 ha), were both analyzed with the same techniques in order to find differences and agreements. The first technique used (Vis-NIR) spectral analysis as a fingerprint, using a partial least squares regression model. A second technique was a quantitative composite fingerprinting technique using chemical analysis of soil and suspended sediment samples. As a comparison, the partial least squares model was also used on the chemical data. In the period of August until September 2009, 30 soil samples of 3 different land uses (landslides, cropland and grazing land) and 21 suspended sediment samples at the catchment outlet were collected. Soil samples were all sieved to <63 μm. Chemical analyses consisted of total element concentration, percentage carbon, percentage nitrogen, atom percentage ^{15}N and $\delta\ ^{13}C$. Reflectance measurements were taken on dried soil samples with a spectrometer.

Results and discussion - Both techniques were not able to predict the contributions of the three land use types. They could only distinguish between landslide and top soil material. The agreements between the results of both techniques were significant for the Unta catchment (R^2=0.80) but not for the Desera catchment (R^2=0.39). The uncertainty of the technique using Vis-NIR reflectance measurements was slightly higher than with the chemical technique. Both techniques revealed that top soil erosion played an important role during storm runoff discharges. Using the partial least squares model for the chemical data revealed that uncertainty can differ a lot when using other statistical techniques.

Conclusions – The quantitative composite fingerprinting technique using spectral signatures from both soil and suspended sediment samples was able to quantify the contribution of two source

materials (landslides and top soil). It provided a faster and more cost effective alternative to the classical procedure.

Keywords Fingerprinting • Landslides • Sediment yield • Suspended sediments • Vis-NIR

1 Introduction

Transport of sediments in rivers may lead to a series of problems such as flooding, siltation of reservoirs and channels, pollution by sediment-fixed contaminants and degradation of aquatic habitats. Therefore there is a need for reliable techniques that allow to determine the source (origin) of that sediment so that target measures can be taken to reduce sediment production. However, the complex interactions of sediment mobilization and delivery and the spatial and temporal variations make these processes difficult to assess. In addition, there are large costs associated with the long-term monitoring of large-scale river basins (Collins and Walling 2004). Traditionally, information on sediment sources has been collected using direct techniques aimed at quantifying sediment losses at the source location. However, spatial and temporal sampling constraints as well as many operational difficulties hamper the reliability of these techniques (Peart and Walling 1986). In this respect, the fingerprinting technique is an indirect technique known to be valuable and effective for sediment source determination in river catchments (Collins et al. 1998; Collins et al. 2001). The technique is based on two main assumptions: first, the potential sources of the river sediment can be discriminated on the basis of their geochemical properties; and secondly, that the measured properties of soil and sediment allow determination of the relative importance of the sources. Several studies have used various chemical and physical sediment properties for fingerprinting sediment sources. A composite fingerprint property in combination with a multivariate mixing model is able to determine the quantitative contribution of the sources, and this procedure has been successfully applied to a range of environments (e.g. Collins et al. 1997, 1998, 2001; Walling et al. 1999; Minella et al. 2008, Motha et al. 2013, Guzman et al. 2013). However, the application of this technique faces some methodological constraints. Cost and labour for the analysis of potential

sediment sources and suspended sediment samples for a range of properties can be very high. Also the statistical procedure does not take into account the inherent variability of the different sediment source properties (Collins and Walling 2002). Another constraint is that the degree of uncertainty associated with the numerical solutions of the mixing model cannot be calculated (Phillips and Gregg 2001, 2003). Though, recent studies have begun to deal with these problems by using a Monte Carlo approach that incorporates source variability (e.g. Franks and Rowan 2000, Small et al. 2002, Motha et al. 2003, Martinez-Carreras et al. 2010abc, Collins et al. 2010ab).

Fingerprinting using visible and near-infrared (Vis-NIR) reflectance measurements may be an alternative method for determining sediment sources in river catchments (e.g. Poulenard et al. 2009; Martinez-Carreras et al. 2010ab; Legout et al. 2013; Evrard et al. 2013). A requirement for using a mixing model to estimate sediment source properties from reflectance measurements is that these reflectance values show linear additive behaviour (Lees 1997). Multiple scattering on different components of a mixture may lead to non-linear behaviour (Keshava and Mustard 2002). Martinez-Carreras et al. (2010b) tested the linearly additive behaviour of three colour parameters calculated from reflectance parameters of artificial mixtures in the visible wavelength range (350-700nm) and observed linearly additive behaviour. A similar testing by Poulenard et al. (2012) showed good linear additive behaviour for Diffuse Reflectance Infrared Fourier Transform Spectroscopy (DRIFTS) in the mid-infrared range. Further testing of this important requirement for other sediment types and wavelengths (NIR) would be desirable before the method can be applied more widely.

Fingerprinting sediment sources using reflectance measurements are coupled with advanced multivariate statistical methods like partial least squares (PLS) regression analysis (Wold et al. 2001; Viscarra Rossel et al. 2006b). PLS regression allows calculating a confidence interval of the predicted sediment contributions. Several recent studies already used reflectance measurements to estimate sediment contributions. The spectral measurements can be used to calculate colour indices (Martinez-Carreras et al. 2010b) or geochemical properties (Martinez-Carreras et al. 2010a) to use in

100 a multivariate mixing model. Several studies used the spectral measurements directly to estimate
101 sediment source contributions using a PLS approach (e.g. Evrard et al 2013, Legout et al. 2013,
102 Poulenard et al. 2009, 2012). It is also possible to use the spectral measurements directly in a mixing
103 model using linear spectral mixture analysis (Somers et al. 2010). However, this technique is not yet
104 implemented in fingerprinting suspended sediments. The study of Evrard et al. (2013) is a first
105 attempt to compare between the chemical and the spectroscopic fingerprinting method using mid-
106 infrared (MIR) spectra. The present study provides a first attempt of comparing the technique
107 between the chemical method and spectra in the Vis-NIR range. An unresolved question is also how
108 uncertainty varies or how uncertainty is influenced regarding to the estimates of sediment source
109 contributions when reflectance measurements using PLS estimates are used instead of classical
110 sediment fingerprinting using mixing model analyses (Martinez-Carreras et al. 2010a).

111 In this study, we examined if Vis-NIR reflectance measurements allow estimating sediment source
112 contributions to sediment yield and compared this with the chemical technique. The two
113 fingerprinting techniques were used to estimate the relative importance of the primary potential
114 sediment sources within two headwater catchments of the Gilgel Gibe river in Southwestern
115 Ethiopia. The first technique used visible and near-infrared signatures as a fingerprint. Here, a PLS
116 regression model was used to calculate the source type contributions. The second technique applied
117 was a quantitative composite fingerprinting technique using chemical analysis of suspended
118 sediment samples and soil samples (potential sediment sources). To quantify the sediment source
119 contributions a numerical mixing model was used in conjunction with the composite fingerprint.
120 Both techniques were compared for agreement, prediction capabilities, useability and practicability.
121 In order to know the influence of the implemented statistical techniques on uncertainty calculation,
122 PLS modeling was also performed on the geochemical fingerprints and compared with PLS modeling
123 of the reflectance measurements.

124

2 Study area

The study area is located in the Gilgel Gibe catchment in Kefa province, Oromiya region, Ethiopia, ca. 260 km southwest of Addis Abeba (Fig. 1). The Gilgel-Gibe catchment is situated on the south-western Ethiopian plateau. The area is strongly influenced by past volcanic activity. It is characterised by a series of basic and subsilicic effusive volcanic rocks, frequently inter-layered with reddish paleosols of Tertiary age (Ministry of Mines and Energy 1997). The rocks found in this area are trachytic or basaltic. The volcanic layers have a gradient of a few degrees in south-western direction and are crossed with fractures and faults. These are related to the main tectonic alignment of the region, the Ethiopian Rift Valley (Ministry of Mines and Energy 1997). The elevation of the Gilgel Gibe catchment is between 1000 and 3300m a.s.l.. It consists of a series of gentle sloping low hills and broad plains surrounded by mountains. The area has a sub-humid climate with an average air temperature of 19.2°C and an average annual rainfall of 1535 mm (Ministry of Mines and Energy 1997). The rainy season covers the months June until October. The two headwater catchments (Unta (2052 ha) and Desera (1657 ha)) are situated about 22 km south of Jimma, near the town of Dedo. The major soil types of the area are Nitisols, Acrisols and Vertisols (FOA-Unesco 1974). Vertisols in the area are limited to flat valley bottoms mostly situated in the lower areas, and did not occur in the two studied catchments. A study of a soil toposequence in the upland area near Dedo town revealed that the studied upland soils were quite similar in their morphological, physical, chemical and mineralogical characteristics (Tolossa 2009). Land use consists mainly of cropland. Some plots are kept as grazing land by the farmers, but such plots are mostly small and surrounded by hedges or tree rows. Forest is only found in the highest regions in the catchment. Total forest cover is only 11%, from which most part is exploited by the farmers (Broothaerts et al. 2012). The region is threatened by landslides which affect the siltation of the Gilgel Gibe dam (Broothaerts et al. 2012). An exploratory study predicted that the dam will be totally filled with sediment within 20 years if the siltation will continue with the current rate, even though the dam was planned to serve for 70 years (Devi et al. 2008).

3 Materials and methods

3.1 Sample collection

Samples from sediment source types were taken from representative areas on different land use. Surface soil samples were taken from grazing land, cropland (Maize *(Zea Mays* L.*),* Barley (*Hordeum Vulgare L.),* Teff *(Eragrostis tef* (Zucc.) Trotter*),* Sorghum *(Sorghum bicolor* (L.) Moench*)* and Wheat *(Triticum aestivum* L.*)*), actively eroding channel banks and landslides using an auger. Care was taken that only material likely to be eroded was sampled: the top 2 cm of grazing lands and croplands, and active landslides exhibiting active erosion. For each catchment (Unta and Desera) 15 soil samples were collected, i.e. 5 from each land use type. This number of samples is rather limited, mainly due to practical reasons, but care was taken to get representative samples from every land use class. Therefore, soil sampling was spread as much as possible over the catchments to capture the variation in sediment sources. For the surface soils of cropland and grazing land, a soil sample consisted of 10 individual samples of the top 2 cm of the soil taken at ca. 10 m intervals on a randomly selected transect to form a composite sample. For the landslides, the samples consisted of material that was situated close (<5 m) to the river. Depth-integrated suspended sediment samples from the rivers were manually taken with a 1.5 l bottle at 4 equidistant positions within the cross-section of the river. The samples were taken at the monitoring stations at the outlet of the catchments. The sediment sample used for further analysis was a composite sample from the four 1.5L samples collected. An effort was made to collect suspended sediment samples at different water heights and on as many times as possible, although at the lowest flows no samples were taken. This was done because sampling at this moment would provide an amount of sediment that is insufficient for fingerprinting analysis, as the sampling was not time integrated. Sediment samples were taken during the rainy season at times when an event occurred. The sampling program ran from 1 August until 30 September 2009. A total of 21 sediment samples were collected.

3.2 Laboratory analysis

All source material soil samples were wet-sieved through a 63 µm mesh, oven-dried at 105°C and manually disaggregated using a pestle and a mortar. Sediment samples were not sieved prior to drying and disaggregation because particle-size analysis of the sediment samples taken during the highest flow rates (and with highest sediment load) indicated they contained little or no sand. The reflectance of the suspended sediment and source samples in the visual and near-infrared (Vis-NIR) light were determined with an ASD LabSpec® Pro spectrometer (Analytical Spectral Devices Inc., Boulder, CO, USA). This mobile instrument has one Si array (350 – 1000 nm) and 2 Peltier cooled InGaAs detectors (1000 - 1800 nm and 1800 - 2500 nm). The sampling interval is 1.4 nm at 350 – 1000 nm and 2 nm at 1000 – 2500 nm. The light source is a quartz-halogen bulb of 3000 K build into the high intensity probe. Every 3 samples a white reference was measured to calibrate the sensor. The spectral properties of the sieved and dried soil and suspended sediment samples were recorded as follows: ± 20 g of soil was transferred into a small disposable petri dish of 1.0 cm height and 3.6 cm diameter. The filled cup was gently tapped on the table, hereafter the surface was carefully levelled with a spatula to obtain maximum reflection. The cup was placed under the sensor as close as possible (3 mm). The diameter of the sensor was 2 cm, resulting in a field of view of 3.14 cm^2. Four separate reflectance readings were taken from each soil specimen by rotating the cups by 90° after each reading. The final spectrum was the average of the four reflectance readings.

The chemical laboratory analysis of both the source material and suspended sediment samples consisted of a range of potential fingerprint properties. Total element concentrations were analysed using a digestion with $LiBO_2$ in graphite crucibles (002380-000 crucible, CML YU40 grade, SCP Science, Quebec, Canada). After the digestion of the soil sample at 1000 °C in a muffle furnace, the melt was dissolved in 50 ml of a 0.42M HNO_3-solution. A 1/10 dilution of this solution was analysed with an ICP-OES (Varian 720ES, Agilent Technologies Inc., Palo Alto, CA, USA) analyser for macro elements (Suhr and Ingamell 1966). Besides total element concentration also percentage carbon (C),

201 percentage nitrogen (N), atom percentage ^{15}N and δ ^{13}C were analysed on the ground samples with
202 an isotope ratio mass spectrometer (ANCA-GSL 20-20, Sercon Limited, Cheshire, UK).

203 ## 3.3 Discriminating catchment sediment sources

204 For all statistical analysis R software was used (R core Team 2013). For both of the methods, the
205 range of concentrations of different properties and wavelengths was tested between the soil
206 samples and the suspended sediment samples according to Walden et al. 1997. If properties or
207 wavelengths of the suspended sediment fell out of the range of the source samples, these were
208 discarded for further analysis.

209 In order to discriminate sediment sources using Vis-NIR spectral measurements, multivariate
210 techniques described by Poulenard et al. (2009, 2012) and Lees (1997) were employed. First,
211 Principal Component Analysis (PCA) was used to determine the natural clustering of samples. This
212 natural clustering was used to investigate if the data was capable of determining sediment source
213 samples by use of the principal components. The PCA scores were then used as input into a
214 Discriminant Analysis.

215 For the chemical method, the two-stage statistical selection procedure described by Collins and
216 Walling (2002) was used to identify the sediment source. In stage one, all individual fingerprint
217 properties were tested for their ability to distinguish between individual source types, using the
218 Kruskal-Wallis H-test. Next, discriminant function analysis was used to identify an optimum
219 composite fingerprint from the fingerprint properties that passed the H-test. Because variables
220 predicting group membership can be strongly correlated, a stepwise selection algorithm was used to
221 select a subset of parameters to predict group membership. The method used was the method of the
222 minimization of Wilk's lambda. If all the group means are the same, a lambda of 1 occurs. A low
223 lambda value means that the variability within the groups is small compared to the total variability
224 (Collins et al. 1998). The stepwise forward variable selection starts with an initial model defined by

the fingerprint property which separates the groups most (lowest lambda). The model is then extended by including extra properties. The selection stops if the *p*-value of including another property is not statistically significant ($p>0.05$).

3.4 Mixing model

The prediction of source type contributions to the sediment samples based on Vis-NIR spectra was assessed using a partial least squares regression (PLSR) model using the package pls (Mevik and Wehrens 2007). Partial least squares regression is a modelling technique usually used for quantitative predictions of sample properties. It is used especially when there are many predictor variables that are strongly correlated. Unlike principal component regression (PCR), it searches for orthogonal factors that maximize the covariance between predictor (X, spectra) and response variables (y, source type contribution). In order to calibrate the partial least squares regression model and to test the linearly additive behaviour of the reflection properties, mixtures of source material samples were made depending on the outcome of the principal component analysis. First, mixtures of pure sources were made, i.e. only soil samples of one source were mixed in the same ratio (Landslide (LS), Grazing land (GL), Cropland (CL)). Then, mixtures of these 'pure' mixtures were made to obtain a range of different source material ratios. These mixtures were then measured with a Vis-NIR spectrophotometer in order to calibrate the model. Model calibration was assessed on individual soil samples, pure mixtures and ratio mixtures as a whole, so that the total variability of soil samples was included in the model. Different pre-treatments of the Vis-NIR data were applied to investigate if they could improve the performance of the model. The pre-treatments that were used were multiplicative scatter correction and standardisation (Stenberg et al. 2010). The first step when selecting a PLSR model is to determine the number of components to include in the model. The optimal number of components gives the best compromise between the description of the calibration set and the model's prediction ability. The PRESS statistic was used to decide which model to use, the optimum number of components is the one with the lowest PRESS statistic. For comparison, also the adjusted coefficient of determination (R^2_{adj}) and the root mean square error of

prediction (RMSEP) were calculated. In order to calculate the PRESS value, a cross validation was performed, using at random 4 or 5 samples as test set. The model was cross validated 10 times, and the ultimate PRESS value was the mean PRESS value of the 10 cross validated models. In order to test the linearly additive behaviour of the spectra, the reflectance spectra of artificial linear mixture samples of source types were computed. The reflectance spectrum of such an artificial sample was calculated as a weighted average of the source samples that were mixed. The spectra of these artificial mixtures were used to calibrate a PLSR model that predicts source type contribution. This model was then applied to the measured (real) mixture samples. If the model predicts the contribution of the source in the mixed samples well, then this reveals the linearly additive behaviour of Vis-NIR spectra.

For the quantification of source contribution to sediment yield using the chemical method a modified numerical mixing model based on that of Collins et al. (2010ab) was used. The basic assumption is that a mixing model relates the fingerprint properties of the suspended sediment samples to the properties of the three possible source samples (landslide, cropland, grazing land):

with being the predicted concentration of the i^{th} fingerprinting property in the suspended sediment sample (e.g. mg/kg or g/kg), S_{ij} the mean concentration of the i^{th} fingerprint property in the source type j (e.g. mg/kg or g/kg) (ls = landslide, g = grazing land, c = cropland) and P_j is the mass fraction of the suspended sediment sample originating from source j. The proportions sum up to one and must have a value between 0 and 1:

For each suspended sediment sample, the proportion was determined by minimizing the sums of squares error (SSE) between the fingerprint property concentrations measured on the suspended sediment sample and those predicted with the mixing model:

where C_i = the measured value of the i^{th} property of the sediment samples (mg/kg or g/kg), P_j = the optimised fraction of sediment contribution, $S_{i,j}$ = the mean concentration of a fingerprint property (mg/kg or g/kg), W_i = a correction factor weighting for the discriminatory power of a certain property, calculated from the scaled H-values of the Kruskal Wallis test of that property, n = number of fingerprint properties and m = number of sediment sources, and $SV_{i,j}$ = a correction factor taking into account the within-source variability of a property (i) in the soil samples of a source category (j). $SV_{i,j}$ is calculated as the inverse of the scaled standard deviation of each property in each source category. This is done using an algorithm proposed by Haskell and Hanson (1981) that is implemented in R by Soetaert et al. (2009). In this calculation no corrections have been made for particle size and organic matter. This is because little is known about the potential errors associated with the use of correction factors for particle size and organic matter (Koiter et al. 2013). The difference in particle size is already minimized by sieving the soil samples to the <63 µm fraction.

When using chemical properties for fingerprinting, there are different types of uncertainties that need to be taken care of when calculating the sediment source contributions. The most important type of uncertainty comes from the use of the mean property values for each sediment source to predict the proportions in the sediment. This mean value is based on a number of samples taken for a given sediment source, and hence subject to sampling error and natural source variability. Therefore, a Monte Carlo approach according to Collins et al. (2010b) was used to translate sampling errors and source variability into uncertainty on the estimated sediment source contribution P_j. Distributions of each fingerprint property for each sediment source were calculated using the median

and robust scale estimator (Q_n) (Rousseeuw and Croux 1993). A total of 5000 numbers ($S_{i,j}$) were picked out of this distribution using a random number generator with a non-negative constraint. These values were then used to solve the mixing model equation a 5000 times to create a 95% confidence interval of the sediment contributions.

In order to better compare the results, because not only different fingerprint properties were used, but also different statistical procedures, partial least squares regression was also performed on the data of the chemical analysis. All data were included that passed the range test, because the PLS regression will decide on the weighing of the parameters that best predict top soil contribution. A partial least squares regression was performed on the chemical dataset predicting source type contribution, only using the data from the pure samples. Here, no mixtures of source samples were analysed chemically. To truly compare the spectra and geochemical tracers under the same conditions, the PLS model of the spectral data was also performed on pure samples, the mixture samples were discarded from the analysis.

4 Results and discussion

4.1 Vis-NIR fingerprinting

4.1.1 Vis-NIR reflectance spectra of soil samples

Fig. 2 shows typical Vis-NIR reflectance spectra for the three types of potential source materials and suspended sediment samples. The spectra of all the samples contain absorption features corresponding to the bending and stretching of OH-bonds of free water. These peaks occur in the near infrared (700-2500 nm) region, at a wavelength of 1400 and 1950 nm. The absorption features at around 2200 nm is characteristic of the AL-OH bend plus O-H stretch of clay minerals like kaolinite and gibbsite. In the visible (400-700 nm) range, reflectance is related to electronic transitions (Viscarra Rossel et al. 2006b) and with minerals containing iron like haematite and goethite (Stenberg et al. 2010). Soil organic matter can also produce broad absorptions in the visible region, due to

317 humic acid. The visible region is different for the landslides compared to that for the grazing and
318 cropland. Landslides were more lightly coloured, because they contain less organic carbon. Fig. 3
319 plots the mean spectra for each source type. The differences in albedo of the spectra can reflect a
320 difference in grain sizes of the soil samples (Stenberg and Viscarra Rossel 2010). Although source
321 material was sieved trough a 63 µm mesh, landslide samples still contained relatively more silt than
322 grazing land and cropland samples. Also the difference in mineralogy between the top soil (grazing
323 land and cropland) and subsoil (landslides) can have an influence on the albedo (Viscarra Rossel et al.
324 2006a). Soil organic carbon is also known to decrease reflectance in the VIS and near to shortwave
325 infrared range (Bayer et al. 2012).

326 *4.1.2 Principal component and discriminant analysis of source materials*

327 PCA was used as an exploratory technique to determine the natural clustering of samples, in order to
328 evaluate overall variability and to find out if sediment sources can be distinguished. Ten principal
329 components explain more than 99% of the variance. The two first principal components of the data,
330 explaining 98.2% of the variability, represent the axes in which the data have the most variability
331 (Fig. 4). From the plot it is clear that landslides can be separated from grazing lands and croplands. A
332 large overlap between grazing lands and croplands exists, even the mean values (centroids) are
333 plotted close to each other. When the scores of the first ten principle components of the PCA were
334 used as input for a discriminant analysis, the groups were more separated (Fig. 5). Although the
335 separation of the 3 source categories is better after discriminant analysis, there is still a large overlap
336 between the grazing and the croplands. All the landslide samples were placed in the right category,
337 but only 7 out of the 10 cropland samples and 8 out of the 10 grazing land samples were correctly
338 classified. In total 83.3% of the samples were predicted to be in the right category. So even after a
339 maximal separation of the groups, a distinction between grazing land and cropland is difficult to
340 make based on reflectance readings. These results indicate that Vis-NIR spectra can be used to
341 determine sediment sources from two types of land uses, i.e. landslides and top soils.

342 *4.1.3 Partial least squares regression model using mixtures*

343 From the PCA analysis it could be concluded that it was not possible to differentiate between grazing
344 land and cropland top soils using Vis-NIR spectra of soils. Therefore a PLSR model was created that
345 considered all top soils (from grazing land and cropland) as one group and predicted the top soil
346 contribution to the suspended sediment. Table 1 represents the mixing scheme per catchment. In
347 total 23 mixtures were made per catchment (Unta and Desera). Mixtures were made to obtain a
348 range of different top soil:landslide ratios, because the PLSR model was in particular intended to
349 predict the top soil contribution in the sediment samples. The model with the lowest PRESS value
350 was chosen as optimal model. The best model was the model with no pretreatment and 8
351 components, it had a PRESS-value of 0.652. If no pre-treatment is used, no correction is made for the
352 albedo differences or scatter of the Vis-NIR spectrum. This means that the albedo difference can be a
353 good predictor of topsoil contribution to suspended sediment. The R^2_{adj} value was 0.947 and the root
354 mean square error of prediction was 0.091. This means that the error of the model is 18%, which is
355 an acceptable error (Fig. 6). This confidence interval is in agreement with Poulenard et al. (2009).

356 Chemometric methods usually are used in chemical analysis to determine the concentration of
357 various chemical compounds. In this study, this approach was used to predict fractions of top soil
358 occurring in suspended sediment samples. Hereby, the linear additive behaviour of the spectra was
359 tested by making artificial linear mixtures of top soil and landslide samples and calibrating a PLS
360 model on those linearly computed mixtures. When the reflectance readings of the mixtures were
361 applied to that model, the fit had a R^2 of 0.97. The good fit shows that the reflectance measurements
362 of the mixtures show linear additive behavior according to the top soil contribution. It shows that the
363 spectrum of a mixed sample is a linear combination of the spectra of pure landslide and pure top soil
364 samples. The partial least squares regression model predicted a range of 15.8 – 70.2% top soil
365 contribution from the Unta catchment and 19.8 – 70.0% top soil contribution from the Desera
366 catchment with a 18.2% error. These measurements indicate that top soil erosion plays an important

role in both catchments. The partial least squares model enabled to calculate a confidence interval for the predictions of sediment sources. Despite its importance, this information is often missing in classical fingerprinting procedures (e.g. Collins et al. 1997ab; Collins et al. 2001; Collins and Walling 2002; Collins and Walling 2004). Only recently, uncertainty associated with sediment source type ascription was assessed using the Monte Carlo approach (e.g. Motha et al. 2003; Collins et al. 2010b; Martinez-Carreras et al. 2010ab) or a likelihood function approach (Minella et al., 2008).

4.1.4 Partial least squares regression model using pure samples

When only pure samples and no mixtures are used to calibrate the PLS model, almost the same performance of the model is acquired. The model with the lowest PRESS value of 0.545 uses 7 components and has an R^2_{adj} of 0.92. The correlation between the predicted contribution of top soil to the suspended sediment with the model using mixtures is 0.98 Unta and 0.99 for Desera. The main difference is that the RMSEP value of the model using pure samples is 0.13. This means that the uncertainty on the prediction rises with 7.8% if only pure samples are used to calibrate the model instead of pure samples and mixtures. It could be argued that with using mixtures the uncertainty is only reduced artificially by adding extra data points in the middle of the regression line. The model based on pure samples only therefore better reflects the uncertainty involved in fingerprinting using spectral measurements.

4.2 Chemical fingerprinting

4.2.1 Chemical analysis of soil samples

The mean concentrations of a range of fingerprint properties measured in the source samples from the Unta and Desera catchment and the results of the Kruskal-Wallis H-test are presented in Table 2. In total, 8 properties passed the test with a critical H-value of 7.38. The results in Table 2 show that a number of selected properties provide a powerful source discrimination. For example, percentage carbon (C) was able to successfully classify 93.3% of all the source samples, followed by percentage

391 nitrogen (N; 83.33%), Manganese (Mn; 80.0%), Aluminium (Al; 66.7%), Zinc (Zn; 66.7%), Zirconium
392 (Zr, 60.0%), atom percentage ^{15}N (56.7%) and $\delta^{13}C$ (50%).

393 There is a small difference in percentage C for grazing lands (3.67%) that is a little bit higher than that
394 for croplands (2.94%), but is highly different from that from landslides (0.65%). This is because
395 landslide material consists mainly of subsoil (weathered rock), which contains little or no carbon
396 from vegetation. The small difference in C between grasslands and croplands is explained by the fact
397 that grasslands in this area are overgrazed, and therefore cannot sequester much C. Also, grazing
398 lands are situated on lands that can no longer be used for crop production. So there is a rotation of
399 alternating land use between cropland and grazing land, so that differences between these two land
400 use types will become less distinct (Smith and Blake 2014). Percentage N follows the same trend as C.

401 There is also no difference in $\delta^{13}C$ measurements for the soils under grazing land and croplands. The
402 dominant crops of the cropland are maize, teff and sorghum, which are C_4-type of plants. Also most
403 tropical grasses have a C_4-type of metabolism. The ranges of the $\delta^{13}C$ values of C_4-type of plants are
404 in between -6 and -19‰, for C_3-type they are in between -24 and -34‰ (Smith and Epstein 1971).
405 The lower value of the landslide samples could be explained by the presence of forest (tree)
406 vegetation, 50 to 100 years ago. Tree species are C_3-types of species, and the roots of the trees could
407 have provided a lower $\delta^{13}C$ value to the subsoil compared to the topsoil of grazing land and cropland.

408 A large difference in concentration of Mn between landslide and top soil samples is measured. Mn
409 has two oxidation states, +II which is more mobile and +IV. The solubility of Mn in soils is mainly
410 affected by pH and redox potential. This normally leads to higher Mn bioavailability in flooded soils.
411 The saturated subsoil of landslides reduces the Mn and makes it more mobile and hence more easily
412 leached. In the top soil of grazing land and cropland Mn retention by cation exchange capacity and
413 ligand exchange reactions will moreover reduce leaching of Mn to the subsoil (Patrick and Turner
414 1968).

Table 3 gives the geochemical and organic matter properties of the suspended sediment samples taken. The range of organic carbon (0.41-3.13%) is situated between that of the source samples, but most sediment samples have values that are quite high. This is possibly due to an enrichment effect of the organic matter associated with the clay content that is related to the sediment transport. Another possible explanation could be that there was another source with a high carbon content

4.2.2 Discriminant function analysis of source materials

The optimum composite fingerprint, given in Table 4, is capable to classify 93.3 % of all the source samples. The fingerprinting properties are not capable of classifying all sediment sources in the right category. This is because there is an overlap between the grazing lands and the croplands. No single property for both sediment source types was different enough to differentiate between the two sources. On the other hand, the difference in fingerprinting properties of landslides with those of the grasslands and croplands was very clear. Because of this, it is better to merge grazing lands and croplands in the same category, i.e. top soils. Now, the source ascription of the sediment is only distinguishing between two main sediment source types i.e. landslides and top soils. This also makes the source ascription more reliable. There would be too much uncertainty in the prediction if three source types would have been used. The Kruskal-Wallis H-test is performed again, now for top soil and landslide as sediment sources. The same composite fingerprint was calculated, now classifying 100 % of all source samples in the right category.

4.2.3 Mixing model

Figs. 7 and 8 show the probability density functions (pdf) of the median contributions from top soils and landslides for the Unta and the Desera catchment as obtained with the chemical fingerprinting technique. The uncertainty because of variation in concentration of properties of the source samples is ranging between 5.4 - 10.7% for the Unta and 4.0 – 9.4% for the Desera catchment. Top soil erosion plays a significant role in the Unta catchment. The contribution of top soil material to the sediment budget is ranging between 3.6 - 59.3%. For the Desera catchment, landslide processes are

440 the dominant processes that contribute to sediment in the river. Here the top soil contribution is
441 ranging between 0.8 -18.4%.

442 A hypothesis is that at low flows, the contribution of the landslides is the highest. Table 5 gives an
443 overview of the sediment samples taken with the corresponding stage height, sediment load and
444 predicted top soil contribution for both methods (Vis-NIR using PLS modeling of mixtures and
445 chemical using the mixing model). The lowest flow measured (52 cm flow depth at the Desera
446 catchment on 15/08/09) corresponds to a contribution of landslides of 99.1 ± 1.9%. This low flow
447 almost corresponds to the base flow in the rainy season. These flows occur in between the rain
448 showers. In this period no soil erosion on cropland or grassland occurs. The only sediment that
449 reaches the river is landslide material, directly connected to the river. Landslides can contribute to
450 river sediment long times after the rain, because then the landslides are still active (Broothaerts et al.
451 2012). At peak flows, more erosion of top soils occurs. Most of the samples are taken directly after or
452 during the rainfall event, mostly at the falling limb of the hydrograph. At these moments, a significant
453 contribution from top soils can be observed. The difference between the Unta and the Desera
454 catchment is that in the Desera catchment, the landslides contribute relatively more to the sediment
455 of the rivers (Broothaerts et al. 2012). The rivers Unta and Desera are very responsive, because the
456 catchment is small, and the topography is undulating. Therefore, the rivers Unta and Desera are
457 narrow and incised and all the sediment that erodes into the stream will directly be transported
458 through the river system. No storage of sediment will take place in the riverbed, only larger stones
459 will stay there. Further downstream, in the broader valleys, storage of sediments will take place.

460 *4.2.4 Partial least squares modeling of chemical fingerprints*

461 The PLS model based on the chemical fingerprints of the soil samples contains 6 components that
462 explain 25.4 % of the variance. The value of the PRESS statistic was 0.778, the R^2_{adj} was 0.88 and the
463 RMSEP was 0.156. The elements with the highest loadings on the first component are Al, Mn, Zn, Zr,
464 %N, atom% 15N, %C and δ 13C ‰. These high loadings correspond to the elements that passed the

Kruskal-Wallis test in the mixing model. The first component explains 9.4% of the variance. In the other components, elements that did not pass the Kruskal-Wallis test like Fe, Ti, V, Cr, Na and Ni have also a high loading. The model predicts a range of top soil contributions for the Unta catchment of 14.7 - 67.9% and for the Desera catchment 11.6 - 46.1%. The correlation between both solution of the mixing model and the PLS model for the chemical fingerprints are 96.1% for the Unta and 90.8% for the Desera catchment. Overall, the PLS model predicts somewhat higher contributions than the mixing model. The main difference is the higher amount of uncertainty for the PLS model, which is 30.2%.

4.3 Comparison of the models

Fig. 9 shows the correlation plots of the results from the two fingerprinting techniques used to assess sediment source ascription in the two catchments. The comparison is made for the PLS model based on reflectance readings using mixtures and for the mixing model based on chemical analysis of the data. For the Unta catchment a correlation coefficient of 0.80 between the two methods is obtained. This means that almost the same results have been achieved using Vis-NIR spectra of sediment samples as compared to the classical technique. For the Desera catchment, the correlation coefficient is only 0.39.

The results achieved by the Vis-NIR method seem to overestimate the contributions of top soil to sediment yield as compared to the classical technique in both catchments. As a control, partial least squares modeling for landslide contribution to the suspended sediment showed that landslide contribution was underestimated compared to the chemical technique (data not shown here), providing thus the same results. For the Desera catchment, the overall estimates of top soil contributions are low (Fig. 9). The range of top soil contribution using the chemical method (0.01 - 0.18) is smaller compared to the Vis-NIR method (0.23 – 0.73). The mixture model of the chemical technique constrains the contributions between 0 and 1 (equation 2). This constraining of the data is needed, because otherwise no useful data would be calculated. Further constraining the

490 contributions with a priori information may reduce uncertainty even more (Collins et al. 2010a). This
491 constraining can only be applied if a clear explanation of the basis for such constraints is given. If
492 these constraints are to be applied with confidence, catchment-specific data has to be used. It can
493 be that due to the constraining, the uncertainty of the solution is estimated as being lower. This
494 constraining can have an influence on the estimation of the uncertainty of the sediment contribution
495 if the contribution is close to 0 or 1. In the plot of the Desera catchment the uncertainty ranges are
496 getting smaller with lower top soil contributions. Normally in linear models, prediction uncertainty
497 will be higher at the extreme values of the regression. Uncertainty of the PLS model is higher because
498 the model was not constrained.

499 In order to know the influence of the statistical technique used, PLS modeling for top soil
500 contribution was also performed on the chemical data. Fig. 10 shows the correlation plot when using
501 the same statistical technique on the different data sets (chemical and spectroscopic). Here, the
502 comparison is made between the PLS model based on reflectance readings using pure samples only
503 and for the PLS model based on chemical fingerprints. For the Unta catchment the correlation
504 coefficient is 0.66 and for Desera 0.52. Overall there is less overestimation for the Unta catchment,
505 but still in the Desera catchment, top soil contribution is overestimated relative to the PLS regression
506 based on the spectroscopic data. The range of top soil contribution is higher for the Desera
507 catchment using a PLS model with chemical fingerprints (12%-46%) compared to the mixing model
508 (1%-18%). Also the two models used different weightings (correction factors) for all parameters.
509 What strikes is the high uncertainty (31%) related to PLS modeling for the chemical data. The main
510 reason for this is that in the calibration procedure only the data from the pure source samples were
511 used having. Here the total variability of the source samples is used to calibrate the model. In the
512 Monte Carlo approach (e.g. Motha et al. 2003, Collins et al. 2010b) the robust scale estimator (Q_n) is
513 used to reflect the uncertainty of the source samples in calculating the contribution. Q_n provides a
514 lower range of values than the total variability. Also, if the PLS model would have been constrained,
515 this would lead to a lower uncertainty value.

516 The mean spectrum of the suspended sediment samples for the Desera catchment (Fig. 2) has a
517 higher albedo than that from the Unta catchment. In the visible region they are positioned closer
518 together than in the near infrared region. The only small difference in the visible region can explain
519 the agreements in percentage top soil contribution from the two catchments, calculated with the
520 Vis-NIR model. This is because a lot of weight is given to the loadings in the visible region of the
521 spectrum of the first component of the PLSR (data not shown here). However, the classical method
522 shows a large difference between the two catchments. Mean percentages of carbon in the
523 suspended sediment are lower in the Desera (1.24%) than in the Unta catchment (1.84%). This can
524 explain the lower top soil contribution in the Desera catchment using the chemical method. The
525 difference of %C is not really reflected in the reflectance measurements of the suspended sediment
526 in both of the catchments, only a little in the NIR region of the spectrum. Validation of the
527 fingerprinting results by erosion measurements can give information on which processes contribute
528 the most sediment to a river. Using different property sets to calculate sediment source ascription
529 probably always will produce somewhat different results. Field observations revealed that a larger
530 area in the Desera catchment is affected by landslides (Broothaerts et al. 2012), supporting the
531 classical analysis. These findings suggest that the Vis-NIR technique somewhat overestimated the
532 contribution of top soil erosion in the Desera catchment. However, a good agreement between the
533 results from both methods in the Unta catchment was achieved. This suggests that visible and near-
534 infrared spectroscopy could be a good alternative technique to predict source type contribution of
535 suspended sediment samples.

536 ## 5 Conclusions

537 This study aimed at comparing fingerprint procedures based on two different techniques: one using
538 chemical analysis of both soil and sediment samples and the other using spectroscopic (Vis-NIR)
539 measurements of those samples. In comparing the spectral measurements with the classical
540 chemical technique with a mixing model, a good agreement between both techniques was found in

one catchment. In another catchment there was little agreement, and the spectroscopic technique systematically overestimated the top soil contribution. We moreover found that Vis-NIR reflectance spectra show linear additive behavior, which is a requirement when using a PLRS model to estimate sediment source contributions.

Predictions of sediment source contributions based on the spectroscopic technique combined with PLS regression had wider confidence intervals than predictions based on the classical chemical technique with a mixing model (and Monte-Carlo sampling to derive confidence intervals). But this difference in uncertainty turned out to be related to the difference in statistical technique (PLS regression vs. mixing model), and not to the type of data it was based on (Vis-NIR spectra vs. geochemical data): When PLS regression was used to estimate sediment source contributions from both types of data, the uncertainty was similar.

Fingerprinting procedures based on spectral reflectance signatures are very attractive because of their simplicity in laboratory analysis. Moreover the costs in both time and equipment compared with the chemical fingerprinting approach are small. Therefore, it provides a good means of assessing suspended sediment source ascription in small river basins, and in particular for situations where many suspended sediment samples need to be analyzed, such as when variation in sediment source during rainfall events is to be examined. Our results confirm that fingerprinting based on Vis-NIRS spectra offers great potential and are comparable to more established techniques like the fingerprinting based on chemical fingerprints.

Acknowledgements This study was conducted in the framework of Soil Fertility project of the IUC-JU, a cooperation between Jimma University (Ethiopia) and different Flemish universities with support from the Flemish Interuniversity Council (VLIR-UOS). The fieldwork was also made possible by a travel grant from VLIR-UOS to the first author. Special appreciation is extended to all members of the VLIR-IUC project for support during the fieldwork. Appreciation is extended to anonymous reviewers, for the critical and helpful comments to an earlier draft of this paper.

566 **References**

567 Broothaerts N, Kissi E, Poesen J, Van Rompaey A, Getahun K, Van Ranst E, Diels J (2012) Spatial
568 patterns, causes and consequences of landslides in the Gilgel Gibe catchment, SW Ethiopia.
569 Catena 97:127–136, doi: 10.1016/j.catena.2012.05.011

570 Bayer A, Bachmann M, Müller A, Kaufmann H (2012) A comparison of feature-based MLR and PLS
571 regression techniques for the prediction of three soil constituents in a degraded South African
572 ecosystem. Appl Environ Soil Sc 2012 (Article ID 971252) 20 pp, doi:10.1155/2012/971252

573 Collins AL, Walling DE, Leeks GJL (1997) Source type ascription for fluvial suspended sediment based
574 on a quantitative composite fingerprinting technique. Catena 29(1):1–27, doi: 10.1016/S0341-
575 8162(96)00064-1

576 Collins AL, Walling DE, Leeks GJL (1998) Use of composite fingerprints to determine the provenance
577 of the contemporary suspended sediment load transported by rivers. Earth Surf Proc Land
578 23(1):31–52, doi: 10.1002/(SICI)1096-9837(199801)23:1<31::AID-ESP816>3.0.CO;2-Z

579 Collins AL, Walling DE, Sichingabula HM, Leeks GJL (2001) Suspended sediment source fingerprinting
580 in a small tropical catchment and some management implications. Appl Geogr 21(4):387–412,
581 doi: 10.1016/S0143-6228(01)00013-3

582 Collins AL, Walling DE (2002) Selecting fingerprint properties for discriminating potential suspended
583 sediment sources in river basins. J Hydr 261(1-4):218–244, doi: 10.1016/S0022-1694(02)00011-2

584 Collins AL, Walling DE (2004) Documenting catchment suspended sediment sources: problems,
585 approaches and prospects. Prog Phys Geog 28(2):159–196, doi: 10.1191/0309133304pp409ra

586 Collins AL, Walling DE, Webb L, King P (2010a) Apportioning catchment scale sediment sources using
587 a modified composite fingerprinting technique incorporating property weightings and prior
588 information. Geoderma 155(3-4):249–261, doi: 10.1016/j.geoderma.2009.12.008

589 Collins AL, Zhang Y, Walling DE, Grenfell SE, Smith P (2010b) Tracing sediment loss from eroding farm
590 tracks using a geochemical fingerprinting procedure combining local and genetic algorithm
591 optimisation. Sci Tot Environ 408(22):5461–5471, doi: 10.1016/j.scitotenv.2010.07.066

592 Devi R, Tesfahune E, Legesse W, Deboch B, Beyene A (2008) Assessment of siltation and nutrient
593 enrichment of Gilgel Gibe dam, Southwest Ethiopia. Bioresource Technol 99(5):975–979, doi:
594 10.1016/j.biortech.2007.03.013

595 Evrard O, Poulenard J, Nemery J, Ayrault S, Gratiot N, Duvert C, Prat C, Lefevre I, Bonte P, Esteves M
596 (2013) Tracing sediment sources in a tropical highland catchment of central mexico by using
597 conventional and alternative fingerprinting methods. Hydrol Process 27(6):911–922, doi:
598 10.1002/hyp.9421

599 FAO-Unesco (1974) FAO/Unesco Soil Map of the World 1:5.000.000, Unesco, Paris

600 Franks SW, Rowan JS, (2000) Multi-parameter fingerprinting of sediment sources: uncertainty
601 estimation and tracer selection. In: Bentley LR (Ed), Comp Met Wat Res XIII. Balkema,
602 Rotterdam, pp. 1067–1074
603 Guzman G, Quinton JN, Nearing MA, Mabit L, Gomez JA (2013) Sediment tracers in water erosion
604 studies: current approaches and challenges. J of Soil Sediment 13(4):816–833, doi:
605 10.1007/s11368-013-0659-5
606 Haskell K, Hanson R (1981) An algorithm for linear least squares problems with equality and
607 nonnegativity constraints. Math Program 21(1):98–118, doi: 10.1007/BF01584232
608 Keshava N, Mustard JF (2002) Spectral unmixing. IEEE Signal Proc Mag 19(1):44–57, doi:
609 10.1109/79.974727
610 Koiter A, Owens P, Petticrew E, Lobb D (2013) The behavioural characteristics of sediment properties
611 and their implications for sediment fingerprinting as an approach for identifying sediment
612 sources in river basins. Earth-Sci Rev 125(0):24 – 42, doi:
613 http://dx.doi.org/10.1016/j.earscirev.2013.05.009
614 Lees JA (1997) Mineral magnetic properties of mixtures of environmental and synthetic materials:
615 linear additivity and interaction effects. Geophys J Int 131(2):335–346, doi: 10.1111/j.1365-
616 246X.1997.tb01226.x
617 Legout C, Poulenard J, Nemery J, Navratil O, Grangeon T, Evrard O, Esteves M (2013) Quantifying
618 suspended sediment sources during runoff events in headwater catchments using
619 spectrocolorimetry. J Soil Sediment 13(8):1478–1492, doi: 10.1007/s11368-013-0728-9
620 Martinez-Carreras N, Krein A, Udelhoven T, Gallart F, Iffly JF, Hoffmann L, Pfister L, Walling DE
621 (2010a) A rapid spectral-reflectance-based fingerprinting approach for documenting suspended
622 sediment sources during storm runoff events. J Soil Sediment 10(3):400–413, doi:
623 10.1007/s11368-009-0162-1
624 Martinez-Carreras N, Udelhoven T, Krein A, Gallart F, Iffly JF, Ziebel J, Hoffmann L, Pfister L, Walling
625 DE (2010b) The use of sediment colour measured by diffuse reflectance spectrometry to
626 determine sediment sources: Application to the Attert river catchment (Luxembourg). J Hydr
627 382(1-4):49–63, doi: 10.1016/j.jhydrol.2009.12.017
628 Martinez-Carreras N, Krein A, Gallart F, Iffly JF, Pfister L, Hoffmann L, Owens PN (2010c) Assessment
629 of different colour parameters for discriminating potential suspended sediment sources and
630 provenance: A multi-scale study in luxembourg. Geomorphology 118(1-2):118–129, doi:
631 10.1016/j.geomorph.2009.12.013
632 Mevik B-H, Wehrens R (2007) The pls Package: Principal Component and Partial Least Squares
633 Regression in R, J Stat Softw 18(2):1—24

634 Minella JPG, Walling DE, Merten GH (2008) Combining sediment source tracing techniques with
635 traditional monitoring to assess the impact of improved land management on catchment
636 sediment yields. J Hydr 348(3-4):546–563, doi: 10.1016/j.jhydrol.2007.10.026
637 Ministry of Mines and Energy (1997) Gilgel Gibe hydroelectric project, environmental assessment,
638 main report. Tech. rep., Ethiopian Electric Light and Power Authority, Addis Abeba, Ethiopia, 100
639 pp
640 Motha JA, Wallbrink PJ, Hairsine PB, Grayson RB (2003) Determining the sources of suspended
641 sediment in a forested catchment in southeastern Australia. Water Resourc Res 39(3):1056, doi:
642 10.1029/2001WR000794
643 Patrick WH, Turner FT (1968) Effect of redox potential on manganese transformation in waterlogged
644 soil. Nature 220(5166):476–478, doi: 10.1038/220476a0
645 Peart MR, Walling DE (1986) Fingerprinting sediment source: the example of a drainage basin in
646 Devon, UK. In: Hadley R (ed) Drainage Basin Sediment Delivery, IAHS Press, Wallingford, IAHS-
647 AISH publication number 159, pp 41–55, http://iahs.info/redbooks/a159/iahs_159_0041.pdf
648 Phillips DL, Gregg JW (2001) Uncertainty in source partitioning using stable isotopes. Oecologia
649 127(2):171–179, doi: 10.1007/s004420000578
650 Phillips DL, Gregg JW (2003) Source partitioning using stable isotopes: coping with too many sources.
651 Oecologia 136(2):261–269, doi: 10.1007/s00442-003-1218-3
652 Poulenard J, Perrette Y, Fanget B, Quetin P, Trevisan D, Dorioz JM (2009) Infrared spectroscopy
653 tracing of sediment sources in a small rural watershed (French Alps). Sci Total Environ
654 407(8):2808–2819, doi: 10.1016/j.scitotenv.2008.12.049
655 Poulenard J, Legout C, Nemery J, Bramorski J, Navratil O, Douchin A, Fanget B, Perrette Y, Evrard O,
656 Esteves M (2012) Tracing sediment sources during floods using Diffuse Reflectance Infrared
657 Fourier Transform Spectrometry (DRIFTS): A case study in a highly erosive mountainous
658 catchment (Southern French Alps). J Hydr 414:452–462, doi: 10.1016/j.jhydrol.2011.11.022
659 R Core Team (2013) R: A Language and Environment for Statistical Computing, R Foundation for
660 Statistical Computing, Vienna, Austria, http://www.R-project.org/
661 Rousseeuw PJ, Croux C (1993) Alternatives to the median absolute deviation. J Am Stat Assoc
662 88(424):1273–1283
663 Small IF, Rowan JS, Franks SW (2002) Quantitative sediment fingerprinting using a Bayesian
664 uncertainty estimation framework. In: Dyer FJ, Thoms MC, Olley JM (Eds), The Structure,
665 Function and Management Implications of Fluvial Sedimentary Systems. IAHS-AISH P No. 276.
666 IAHS Press, Wallingford, pp. 443–450
667 Smith BN, Epstein S (1971) 2 categories of C^{13}/C^{12} ratios for higher plants. Plant Physiol 47(3):380–
668 384

669 Smith HG, Blake WH (2014) Sediment fingerprinting in agricultural catchments: A critical re-
670 examination of source discrimination and data corrections. Geomorphology 204:177–191, doi:
671 10.1016/j.geomorph.2013.08.003
672 Soetaert K, Van den Meersche K, van Oevelen D (2009) limSolve: Solving Linear Inverse Models. R-
673 package version 1.5.1
674 Somers B, Delalieux S, Verstraeten W, Van Aardt J, Albrigo G, Coppin P (2010) An automated
675 waveband selection technique for optimized hyperspectral mixture analysis. Int J Remote Sens
676 31(20):5549-5568, doi:10.1080/01431160802304625
677 Stenberg B, Viscarra Rossel RA (2010) Diffuse reflectance spectroscopy for high-resolution soil
678 sensing. In: Viscarra Rossel RA, McBratney AB, Minasny B (eds) Proximal Soil Sensing, Progress
679 in Soil Science, vol 1, Springer Netherlands, pp 29–47, doi: 10.1007/978-90-481-8859-8_3
680 Stenberg B, Viscarra Rossel RA, Mouazen AM, Wetterlind J (2010) Visible and near infrared
681 spectroscopy in soil science. Adv Agron 107:163–215, doi: 10.1016/S0065-2113(10)07005-7
682 Suhr NH, Ingamell CO (1966) Solution technique for analysis of silicates. Anal Chem 38(6):730–734
683 Tolossa AR, Deckers S, Van Ranst E (2009) Formation and characteristics of Nitisols and the
684 transformation of Nitic into Ferralic Properties in South-West Ethiopia. Master thesis
685 dissertation, University of Gent and Vrije Universiteit Brussel, 106pp
686 Viscarra Rossel RA, McGlynn R, McBratney A (2006a) Determining the composition of mineral-
687 organic mixes using UV-vis-NIR diffuse reflectance spectroscopy. Geoderma 137(1-2):70–82,
688 doi: http://dx.doi.org/10.1016/j.geoderma.2006.07.004
689 Viscarra Rossel RA, Walvoort DJJ, McBratney AB, Janik LJ, Skjemstad JO (2006b) Visible, near infrared,
690 mid infrared or combined diffuse reflectance spectroscopy for simultaneous assessment of
691 various soil properties. Geoderma 131(1-2):59–75, doi: 10.1016/j.geoderma.2005.03.007
692 Walden J, Slattery MC, Burt TP (1997) Use of mineral magnetic measurements to fingerprint
693 suspended sediment sources: approaches and techniques for data analysis. J Hydr 202(1-
694 4):353–372, doi: 10.1016/S0022-1694(97)00078-4
695 Walling DE, Owens PN, Leeks GJL (1999) Fingerprinting suspended sediment sources in the
696 catchment of the River Ouse, Yorkshire, UK. Hydrol Process 13(7):955–975, doi:
697 10.1002/(SICI)1099-1085(199905)13:7<955::AID-HYP784>3.0.CO;2-G
698 Wold S, Sjostrom M, Eriksson L (2001) PLS-regression: a basic tool of chemometrics. Chemometrics
699 and Intelligent Laboratory Systems 58(2):109–130, doi: 10.1016/S0169-7439(01)00155-1

700 **Table 1** Composition of the soil sample mixtures used to calibrate the PLSR model. This table
701 represents the mixing scheme for one catchment. Identical mixtures were produced for both the
702 Unta and the Desera catchments (LS = landslide, CL=cropland and GL= grazing land)

Sample label	Weight percentage of the classes of source material				
	Landslide material	Cropland top soil	Grazing land top soil	Total top soil	Total Landslide
Pure Mixtures					
LS	100			0	100
GL			100	100	0
CL		100		100	0
Ratio Mixtures					
LS CL 10 90	10	90		90	10
LS CL 25 75	25	75		75	25
LS CL 50 50	50	50		50	50
LS CL 75 25	75	25		75	25
LS CL 90 10	90	10		10	90
LS GL 10 90	10		90	90	10
LS GL 25 75	25		75	75	25
LS GL 50 50	50		50	50	50
LS GL 75 25	75		25	75	25
LS GL 90 10	90		10	10	90
LS CL GL 10 10 80	10	10	80	90	10
LS CL GL 10 80 10	10	80	10	90	10
LS CL GL 25 25 50	25	25	50	75	25
LS CL GL 25 50 25	25	50	25	75	25
LS CL GL 33 33 33	33	33	33	67	33
LS CL GL 80 10 10	80	10	10	20	80
LS CL GL 50 25 25	50	25	25	50	50

703

Table 2 The ability of individual fingerprint properties to distinguish sediment source type, assessing the Kruskal-Wallis H test and discriminant function analysis (DFA). Al: Aluminium; As: Arsenic; Ba: Barium; Ca: Calcium; Cr: Chromium; Cu: Copper; Fe: Iron; K: Potassium; Mg: Magnesium; Mn: Manganese; Na: Sodium; Ni: Nickel; P: Phosphorus; Sc: Scandium; Si: Silicium; Sr: Strontium; Ti: Titanium; V: Vanadium; Zn: Zinc; Zr: Zirconium

	Mean Concentration						Kruskal-Wallis			DFA[c]
Fingerprint Property	Landslides		Cropland		Grazing land		H-Value[a]	*P*-Value	Significance[b]	Correctly classified samples (%)
	Mean	CV (%)	Mean	CV (%)	Mean	CV (%)				
Al g/kg	117	10	90	13	87	14	19.38	<0.001	***	67
As mg/kg	26	27	29	36	29	56	0.20	0.904		
Ba mg/kg	392	36	385	12	380	23	0.28	0.869		
Ca g/kg	6.19	85	3.80	33	3.41	31	1.44	0.486		
Cr mg/kg	142	71	117	37	138	57	0.07	0.965		
Cu mg/kg	35	46	35	22	34	22	0.29	0.865		
Fe g/kg	85.2	21	92.9	18	86.3	18	2.39	0.303		
K g/kg	8.14	79	8.33	24	7.78	33	0.64	0.727		
Mg g/kg	7.19	56	5.12	37	4.41	28	4.66	0.097		
Mn g/kg	1.13	31	3.24	20	3.20	20	19.40	<0.001	***	80
Na g/kg	6.86	111	3.85	26	3.87	35	0.06	0.968		
Ni mg/kg	89	63	71	32	80	41	0.84	0.658		
P g/kg	1.43	62	1.17	14	1.16	18	0.01	0.995		
Sc mg/kg	22	27	18	28	17	35	5.27	0.072		
Si g/kg	198	10	201	9	202	11	0.26	0.879		
Sr mg/kg	112	67	67	28	66	36	4.86	0.088		
Ti g/kg	14.6	28	15.9	30	13.8	36	1.56	0.459		
V mg/kg	214	35	238	33	199	37	2.52	0.284		
Zn mg/kg	146	18	224	14	214	15	16.85	<0.001	***	67
Zr mg/kg	485	38	1054	24	1083	23	16.85	<0.001	***	60
%N	0.05	59	0.28	12	0.35	15	22.43	<0.001	***	83
atom% ^{15}N	0.38	0	0.38	0	0.38	0	12.16	0.002	**	57
%C	0.65	56	2.94	10	3.67	14	23.08	<0.001	***	93
$\delta^{13}C$ ‰	-22.38	9	-19.27	7	-19.11	6	12.31	0.002	**	50

[a] Critical H-Value = 7.38 [b] * = $P<0.05$, **=$P<0.01$, ***=$P<0.001$ [c] DFA = Discriminant Function Analysis

Table 3 Mean geochemical and organic matter properties of the suspended sediment samples. Al: Aluminium (g/kg); Ba: Barium (mg/kg); Ca: Calcium (g/kg); Cr: Chromium (mg/kg); Cu: Copper (mg/kg); Fe: Iron (g/kg); K: Potassium (g/kg); Mg: Magnesium (g/kg); Mn: Manganese (g/kg); Na: Sodium (g/kg); Ni: Nickel (mg/kg); P: Phosphorus (g/kg); Sc: Scandium (mg/kg); Si: Silicium (g/kg); Sr: Strontium (mg/kg); Ti: Titanium (g/kg); V: Vanadium (mg/kg); Zn: Zinc (mg/kg); Zr: Zirconium (mg/kg)

Date	Catchment	Al	Ba	Ca	Cr	Cu	Fe	K	Mg	Mn	Na	Ni	P	Sc	Si	Sr	Ti	V	Zn	Zr	%N	atom% ^{15}N	%C	δ ^{13}C ‰
14/08/09	Unta	107	523	11.3	181	40.2	92.3	10.19	8.08	2.93	7.58	95.5	1.76	20.1	217	136	11.8	171	276	799	0.23	0.3683	2.16	-20.99
20/08/09	Unta	98	419	7.8	116	35.3	77.5	10.80	6.21	2.28	6.37	70.7	1.72	15.1	225	101	9.7	141	273	949	0.42	0.3686	3.13	-22.01
22/08/09	Unta	113	554	14.0	206	35.2	98.7	8.29	9.80	2.25	8.04	110.7	1.74	25.2	206	166	13.3	186	216	549	0.15	0.3691	0.79	-22.38
30/08/09	Unta	112	413	11.3	141	45.4	79.8	8.87	8.68	1.64	8.00	100.8	1.57	25.2	208	136	10.3	146	368	675	0.36	0.3691	2.08	-22.09
31/08/09	Unta	112	429	10.5	141	35.3	82.8	9.24	7.98	1.84	7.09	85.8	1.54	20.2	211	136	11.1	162	379	803	0.27	0.3694	2.04	-21.74
02/09/09	Unta	111	434	8.4	172	40.4	87.0	8.69	8.84	2.12	5.69	101.0	1.47	25.3	217	116	13.3	177	187	697	0.15	0.3695	1.36	-19.93
02/09/09**P**	Unta	105	443	8.7	171	35.3	84.7	8.92	7.60	2.10	6.43	90.7	1.72	20.2	217	111	11.2	166	212	655	0.23	0.3689	2.04	-22.62
05/09/09	Unta	110	501	10.8	248	40.5	106.0	8.19	10.67	2.57	7.17	126.6	1.70	25.3	210	137	14.1	198	208	593	0.12	0.3696	0.96	-21.80
07/09/09	Unta	108	440	11.0	142	40.4	84.4	10.04	8.40	2.09	7.48	96.0	1.61	20.2	209	131	10.4	162	329	824	0.28	0.3698	2.16	-21.40
08/09/09	Unta	112	455	8.7	157	40.4	85.4	8.94	7.36	1.94	5.97	85.9	1.75	20.2	215	116	11.3	167	242	743	0.24	0.3690	1.95	-22.14
10/09/09	Unta	108	471	9.2	172	35.4	90.9	10.17	7.74	2.27	7.64	91.1	1.51	20.2	219	127	12.4	177	197	744	0.17	0.3689	1.54	-20.78
14/08/09	Desera	97	397	10.6	65	20.1	80.4	18.06	7.42	1.91	16.10	40.3	1.51	20.1	233	126	9.8	156	201	553	0.19	0.3687	1.70	-22.57
15/08/09	Desera	114	545	10.6	35	20.2	96.0	9.55	9.64	1.66	7.55	30.3	2.44	25.2	201	156	18.3	247	192	429	0.08	0.3694	0.41	-21.98
20/08/09	Desera	93	252	6.1	40	10.1	56.3	25.61	3.91	1.38	23.07	25.2	1.06	15.1	256	66	7.1	86	197	611	0.21	0.3686	1.82	-23.37
22/08/09	Desera	98	349	11.4	56	10.1	67.5	22.65	6.82	1.22	22.38	30.4	1.33	15.2	245	132	8.9	111	192	465	0.14	0.3692	0.82	-23.48
02/09/09**P**	Desera	101	411	8.3	76	25.3	80.6	16.34	6.94	1.84	13.45	50.7	1.44	20.3	230	117	11.6	152	162	563	0.14	0.3693	1.33	-21.67
02/09/09	Desera	97	217	9.7	40	10.1	51.5	25.95	4.92	0.92	25.12	25.3	0.81	15.2	249	91	5.7	61	243	667	0.13	0.3695	1.05	-23.11
05/09/09	Desera	101	303	7.8	56	15.2	64.3	23.51	5.13	1.23	22.09	90.9	1.22	15.2	251	91	7.8	101	177	540	0.27	0.3693	1.38	-23.97
07/09/09	Desera	96	358	8.2	96	20.1	76.0	16.22	6.56	1.51	13.47	60.4	1.23	20.1	230	106	10.9	151	176	589	0.12	0.3686	1.22	-25.65
08/09/09	Desera	100	232	5.1	35	5.0	53.8	25.50	3.38	1.13	22.56	20.2	0.96	15.1	251	60	6.1	65	146	579	0.14	0.3697	1.27	-22.71
10/09/09	Desera	104	272	7.2	55	15.1	58.1	23.57	4.90	1.07	21.26	40.3	0.96	15.1	247	81	7.2	91	217	564	0.14	0.3684	1.44	-24.37

712 **Table 4** Results of the stepwise discriminant function analysis for identifying an optimum composite
713 fingerprint for discriminating source types (landslide, grazing land, cropland)
714

Step	Fingerprint Property	Wilks lambda	Correctly classified samples (%)
1	%C	0.07676	93.3
2	%C + Mn	0.06058	90.0
3	%C + Mn + Zr	0.05066	93.3

715 **Table 5** Stage height, sediment concentration and predicted top soil contribution of the suspended
716 sediment samples taken. Two samples were taken on 02/09/2009, and the record marked with 'P'
717 after the date indicates the sediment sample was taken during peak flow. Stage height readings were
718 recorded at a bridge further downstream were Unta and Desera have merged.

	Unta				Desera			
Date	Stage Height (cm)	Sediment conc. (g/l)	Top soil contribution (%)		Stage Height (cm)	Sediment conc. (g/l)	Top soil contribution (%)	
			Vis-NIR	Chemical			Vis-NIR	Chemical
14/08/09	85	4.59	54.9	41.7	85	4.63	70.0	18.4
15/08/09					52	4.89	43.2	0.9
20/08/09	62	1.49	70.2	59.3	62	2.95	41.8	15.2
22/08/09	62	3.11	17.6	3.7	62	3.49	64.7	2.7
30/08/09	58	0.64	15.8	24.5				
31/08/09	60	0.70	33.8	29.2				
02/09/09	98	4.27	23.0	14.2	80	13.36	37.5	4.7
02/09/09**P**	80	5.52	48.5	29.4	98	49.39	49.9	11.4
05/09/09	70	2.91	22.2	6.1	70	2.09	19.8	4.8
07/09/09	64	0.74	32.2	35.5	64	0.74	44.1	10.6
08/09/09	65	2.31	53.9	27.8	65	4.04	43.8	5.7
10/09/09	80	5.17	44.0	19.8	80	4.06	44.0	5.4

719

720 **Figure captions**

721

722 **Fig. 1** Location of the Gilgel Gibe Catchment and the headwater catchments Unta and Desera. The
723 suspended sediment monitoring stations, top soil and landslide samples are indicated on the map.

724

725 **Fig. 2** Typical spectra from different types of source materials and suspended sediment samples in
726 the Unta (full line) and Desera (dashed line) catchment. Individual samples are plotted in grayscale,
727 mean spectra are black.

728

729 **Fig. 3** Mean spectrum from different type of source materials in the Unta and Desera catchment

730 **Fig. 4** Plot of the first two principal components from the PCA analysis of the VIS-NIR spectra of the
731 source samples (Unta and Desera samples)

732 **Fig. 5** Plot of the first two linear discriminants from the linear discriminant analysis (LDA) using the
733 PCA scores as input (Unta and Desera samples)

734 **Fig. 6** Calibration plot of the PLS modelling for top soil contribution of the mixed samples. The grey
735 dashed line is the 95% prediction interval.

736 **Fig. 7** Probability density functions for the predicted median contributions from each source type to
737 sediment yield in the Unta catchment using the chemical technique. Results are given for suspended
738 sediment samples taken at different dates. P in one day (02/09/2009) indicates sediment sample was
739 taken during peak flow

740 **Fig. 8** Probability density functions for the predicted median contributions from each source type to
741 sediment yield in the Desera catchment using the chemical technique. Results are given for
742 suspended sediment samples taken at different dates. P in one day (02/09/2009) indicates sediment
743 sample was taken during peak flow

744

745 **Fig. 9** Correlation between results from the chemical method using a mixing model and the Vis-NIR
746 method using mixtures in both catchments (Unta and Desera) used for fingerprinting. Bars indicate
747 the uncertainty related to each technique.

748

749 **Fig. 10** Correlation between results from the PLS model using the chemical data and the Vis-NIR data
750 only using pure samples for both catchments (Unta and Desera) used for fingerprinting. Bars indicate
751 the uncertainty related to each technique.

752

753

754 Fig 1

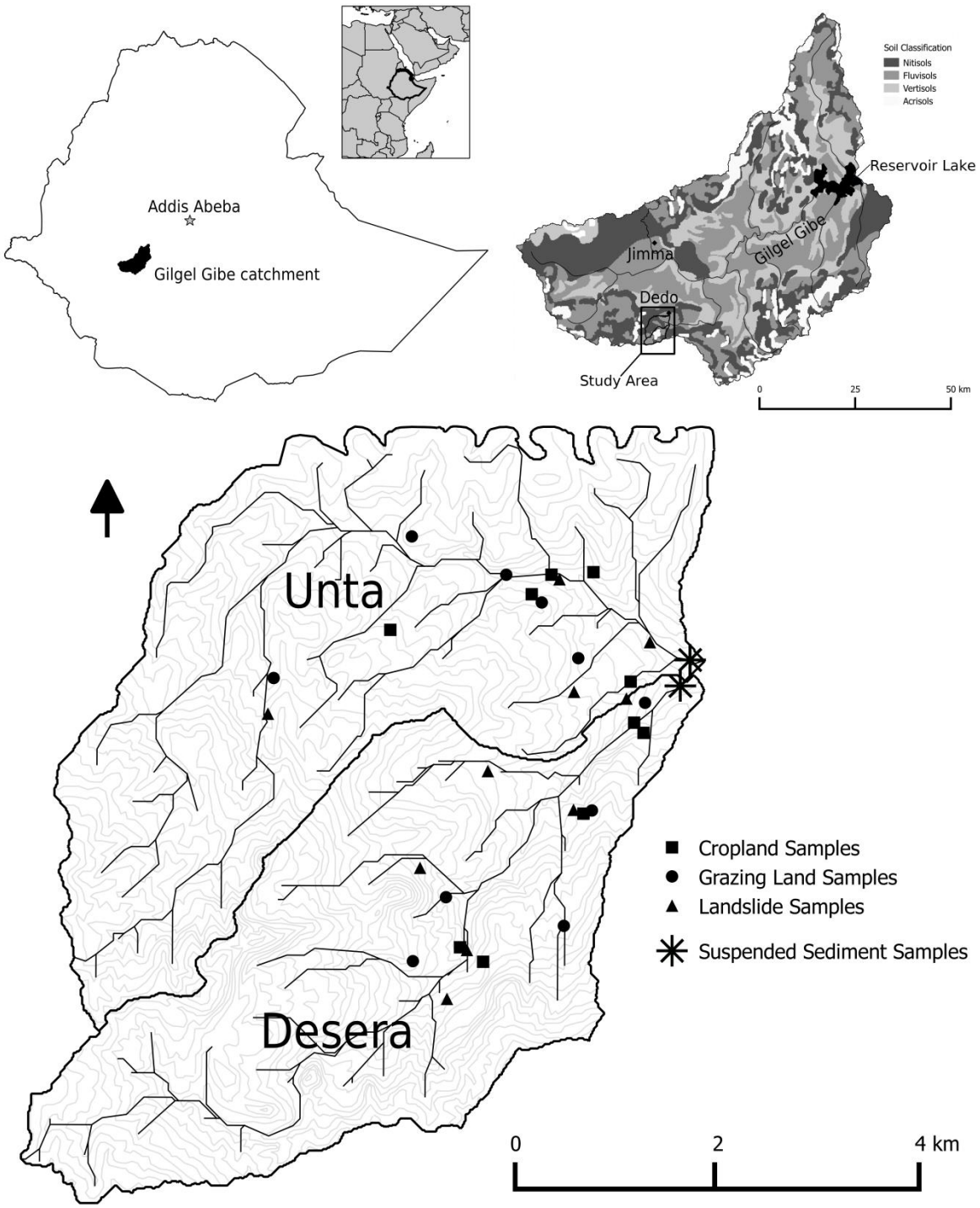

755

756

757

758 Fig 2

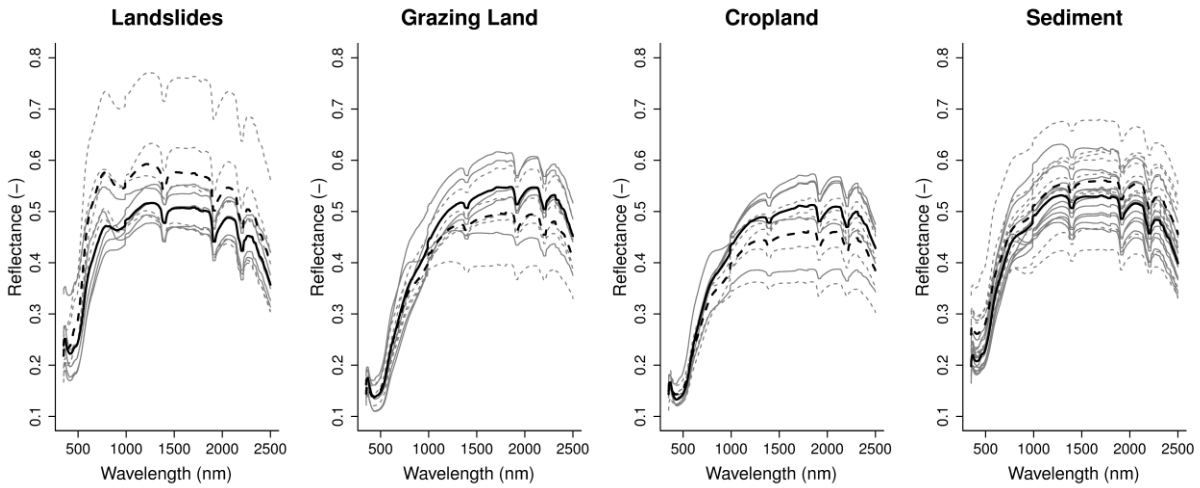

759

760

761

762 Fig 3

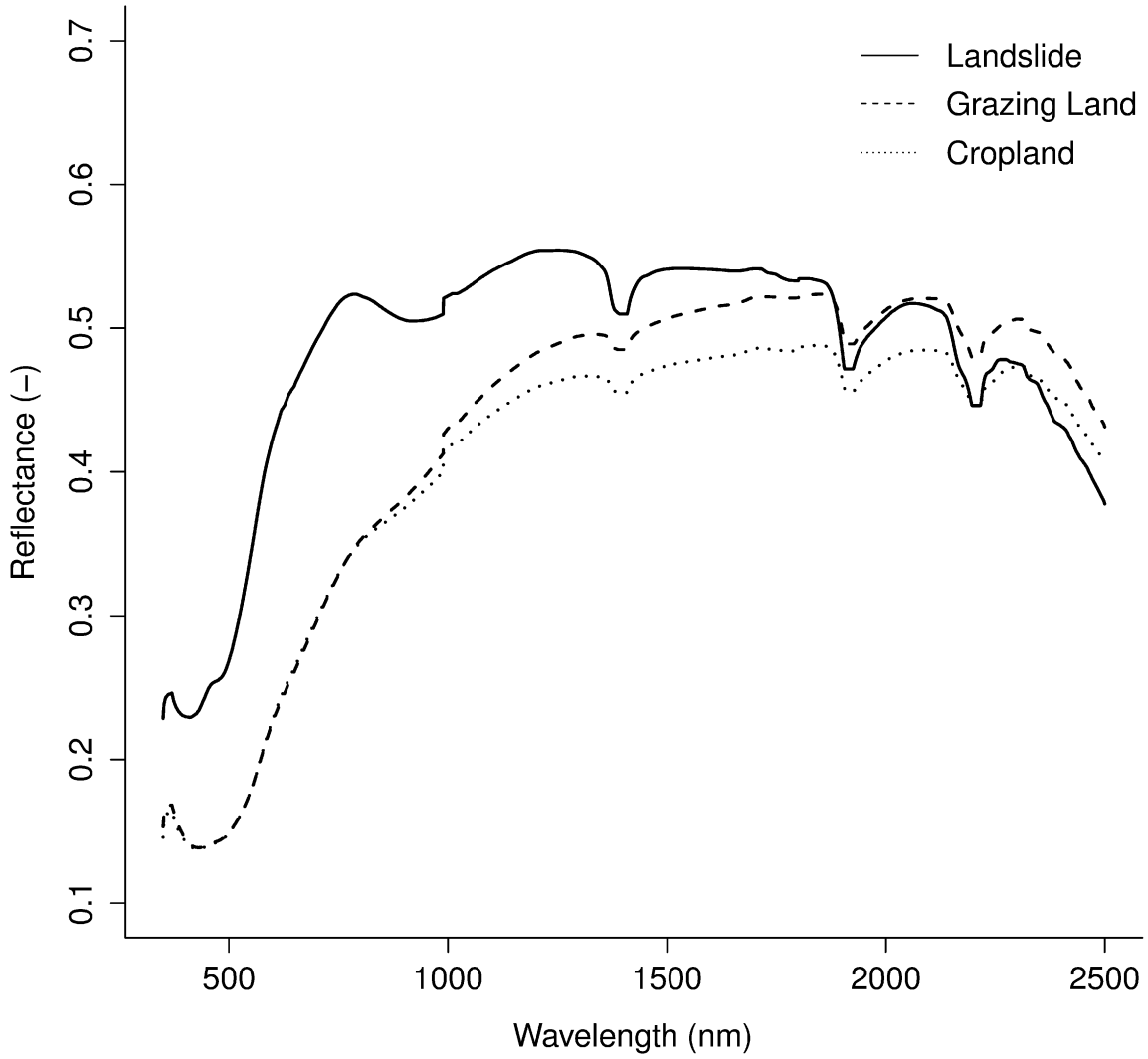

763

764

765

766 Fig 4

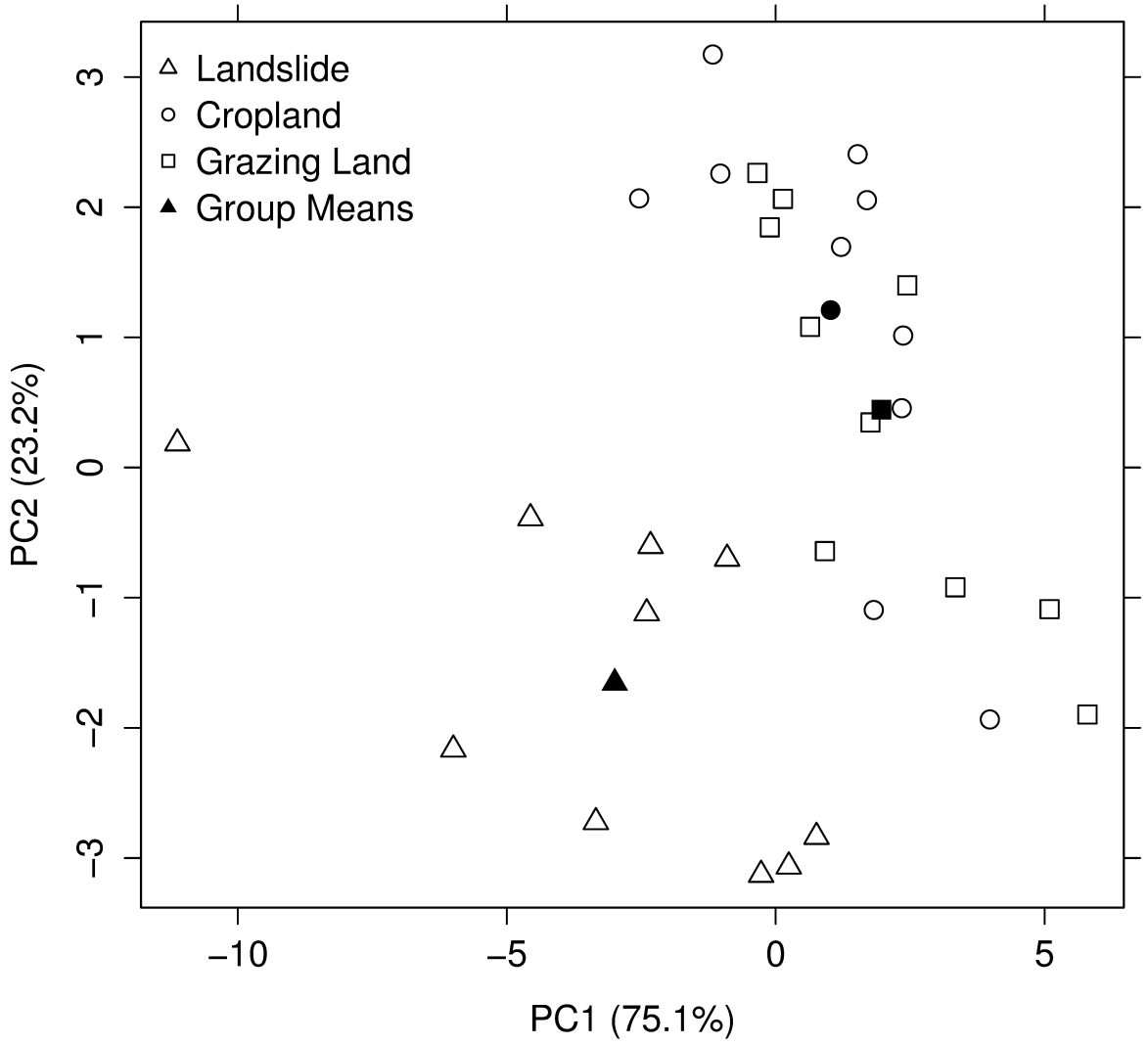

767

768

769 Fig 5

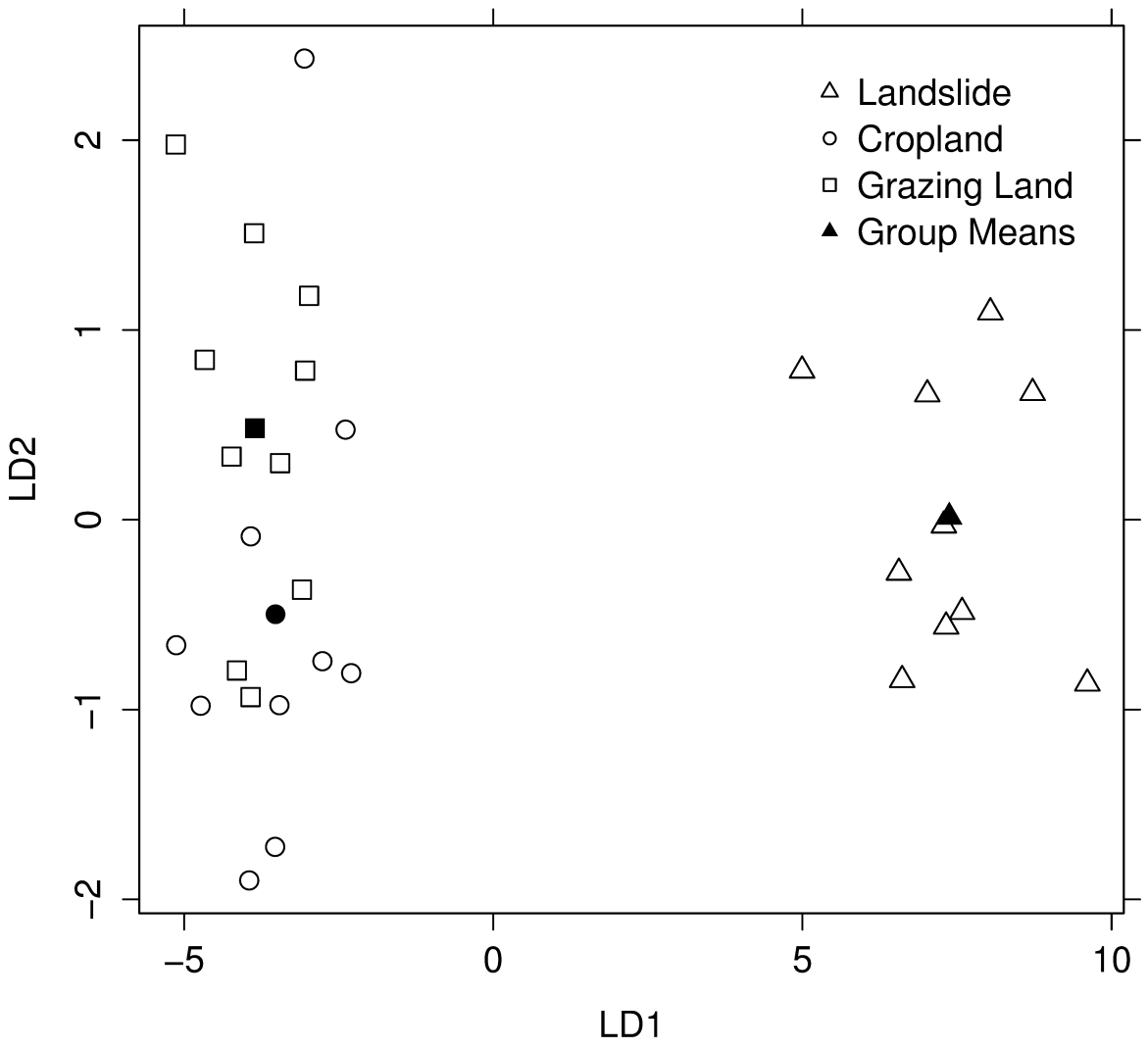

770

771

772

773 Fig 6

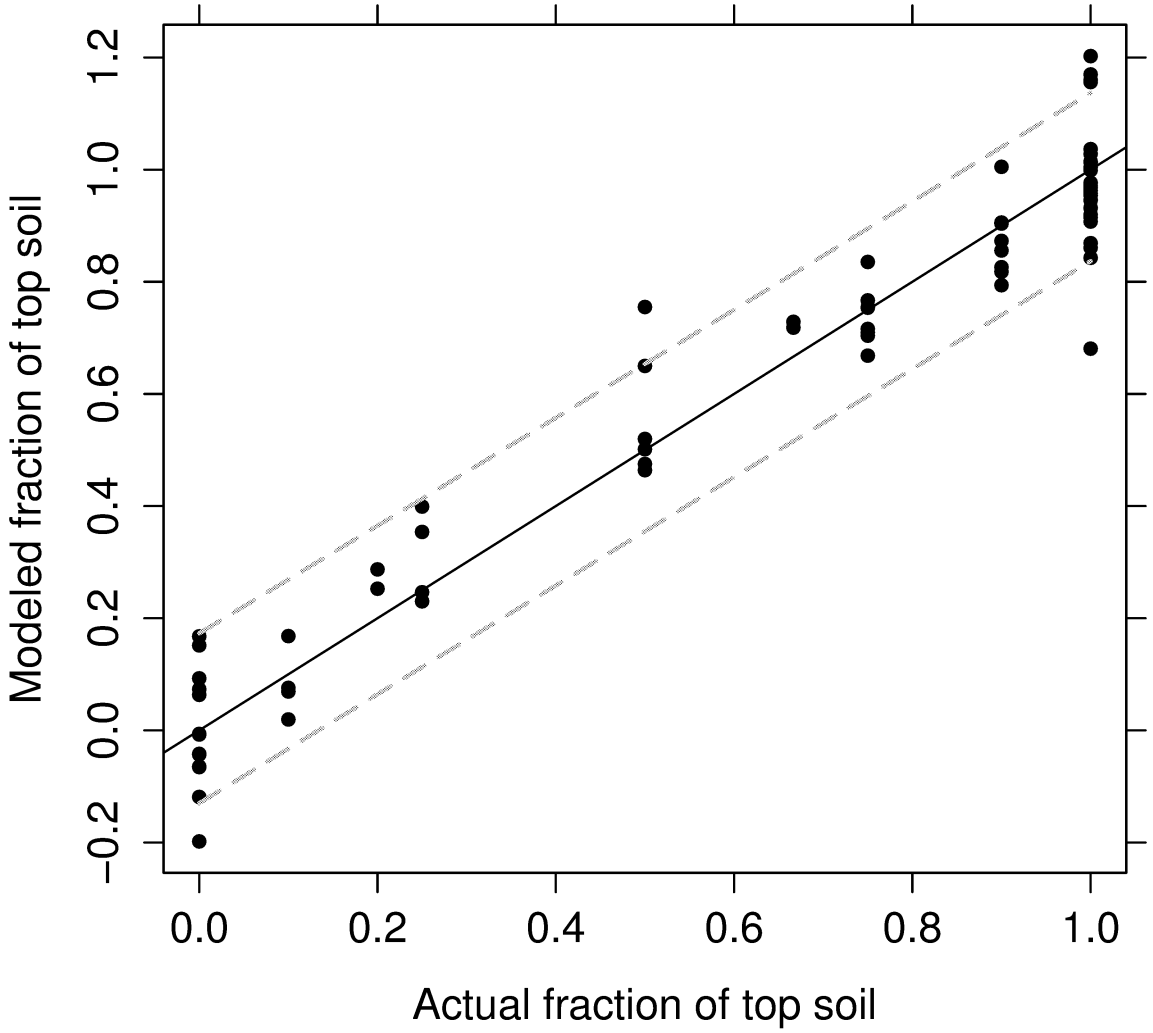

774

775

776

777 Fig 7

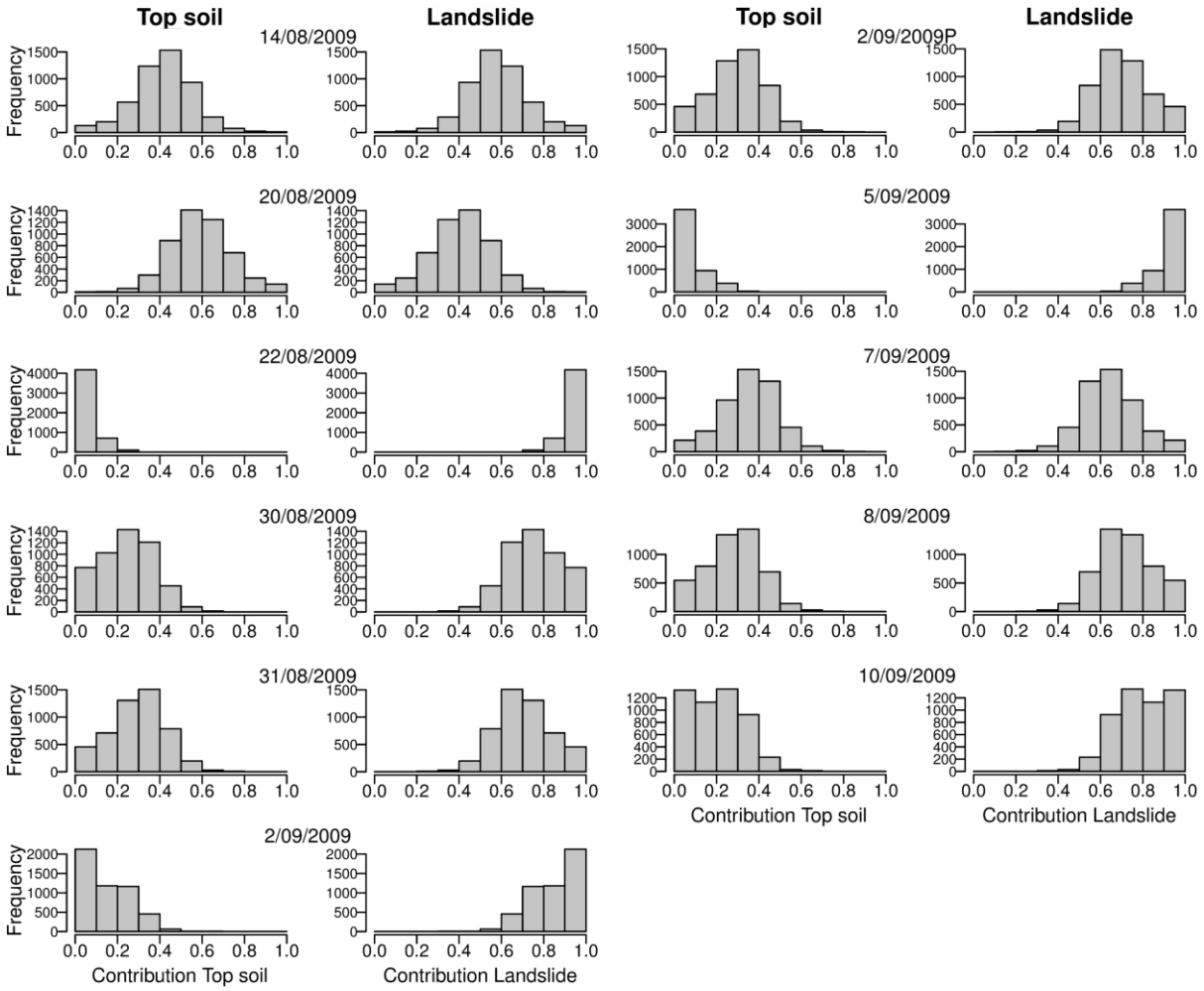

778

779

780 Fig 8

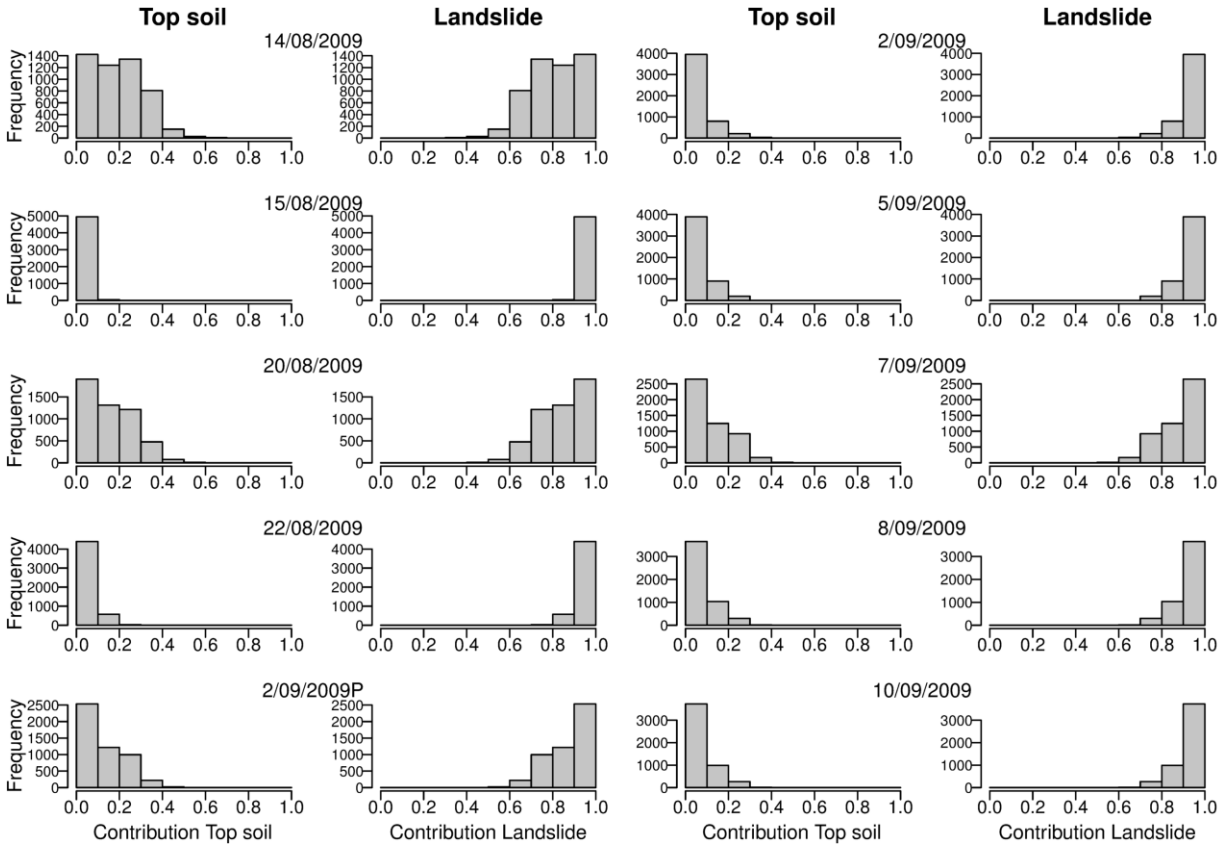

781

782

783

784 Fig 9

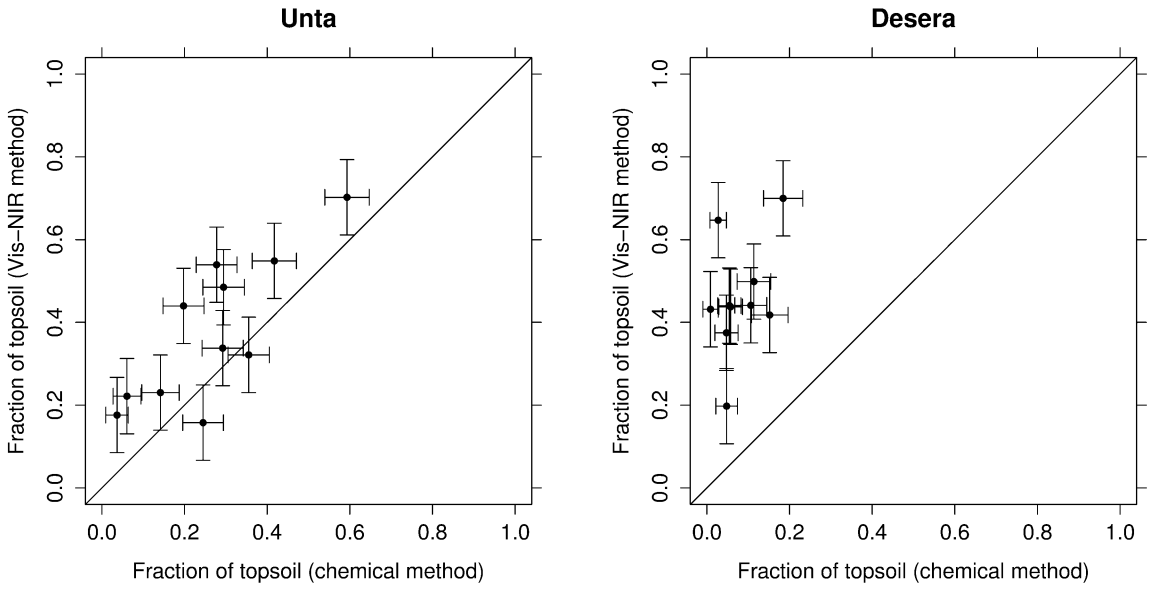

785

786

787

788 Fig 10

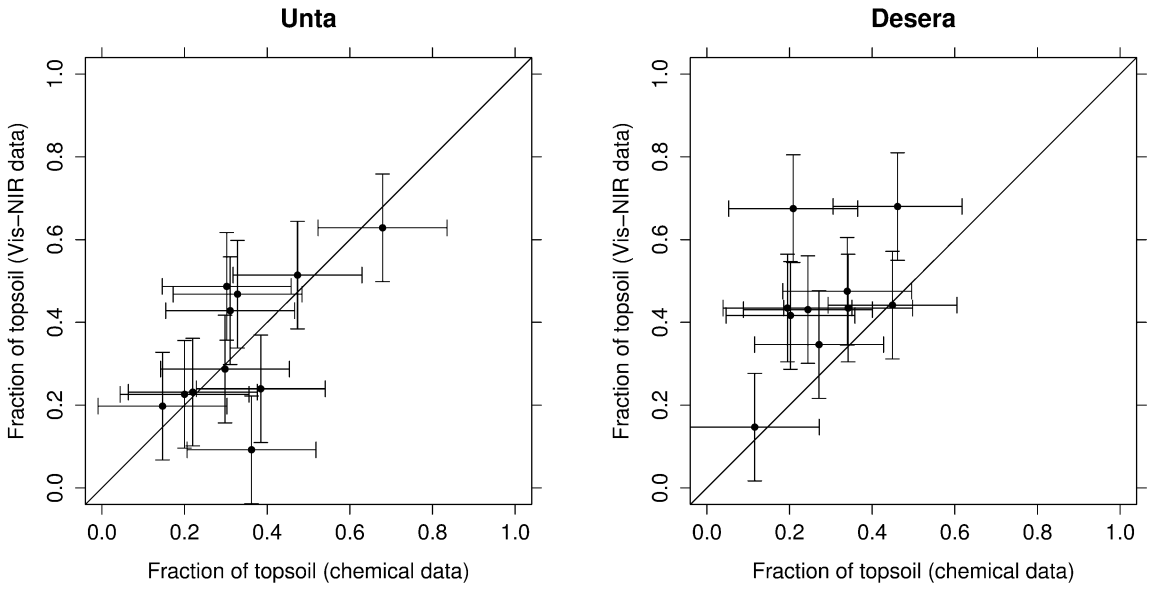

789